In situ grazing incidence small-angle x-ray scattering real-time monitoring of the role of humidity during the structural formation of templated silica thin films

Alain Gibaud, Sandrine Dourdain, Oleg Gang, Benjamin Ocko

PHYSICAL REVIEW B **70**, 161403(R) (2004)

In situ grazing incidence small-angle x-ray scattering real-time monitoring of the role of humidity during the structural formation of templated silica thin films

Alain Gibaud and Sandrine Dourdain
Laboratoire P.E.C., Université du Maine, Faculté des Sciences, 72085 Le Mans Cedex 09, France

Oleg Gang and Benjamin M. Ocko
Department of Physics, Brookhaven National Laboratory, Upton, New York 11973, USA
(Received 26 April 2004; revised manuscript received 22 July 2004; published 25 October 2004)

The role of RH (relative humidity) during the formation of templated silica thin films has been investigated using real-time grazing incidence small-angle x-ray scattering. A detailed analysis of the evolution of the lattice parameters as a function of RH is presented. It is shown that in the modulable steady state, the lattice parameter parallel to the surface is pinned after a transient regime is reached while the parameter normal to the surface can still vary. In the initial stage we find that the film can take up to one layer of water per micelle. Interferometric measurements confirm that swelling occurs in the entire film. An explanation of the pinning effect is presented.

DOI: 10.1103/PhysRevB.70.161403 PACS number(s): 68.55.−a, 61.10.−i

Mesostructured organic assemblies are now routinely used as templates in materials synthesis.[1,2] This approach is based on the tendency of amphiphilic organic molecules to self-organize in aqueous media into complex one-, two-, or three-dimensional supramolecular aggregates. The resulting architectures are used to direct the formation of inorganic solids from soluble precursors.[3–8] Such an organic templating approach to materials synthesis is inspired by the strategies that living organisms utilize to construct bioinorganic materials. Although in all living systems, the role of water is considered to be of paramount importance, there is little known about how amphiphilic molecules self-assemble and eventually reorganize during the evaporation of a solvent under controlled relative humidity (RH). Penetrating probes such as x-ray or neutron radiation used under grazing inidence can provide essential information about liquids and buried interfaces. Using grazing incidence small-angle x-ray scattering (GISAXS), the group of Sanchez and co-workers has recently shown that RH strongly influences the final mesostructure of dip-coated thin films prepared by EISA (evaporation-induced self-assembly).[9–11] In the EISA, the evaporation of the solvent at the interface leads to a concentration gradient that may give rise to structures different at the top and at the bottom of the films.[12,13] Here we report simultaneous GISAXS and multiwavelength optical interferometry measurements during the EISA process and as a function of RH. Whereas the symmetry and lattice parameters are measured with GISAXS, the overall film thickness is obtained from the interferometry. For thin films, the time scale for self-assembly is usually extremely short and transient measurements require both a synchrotron source and a two-dimensional (2D) detector. The combination of these two techniques provides a comprehensive model of how water is incorporated into the silica network during RH cycling. The highly organized structures obtained after complete solvent evaporation are influenced by the external RH. Water intrusion starts at the surface of the films and diffuses towards the substrate producing strong modifications of the lattice parameters.

A sol containing surfactant, silica precursor, ethanol, water, and hydrochloric acid (initial molar composition 1 TEOS (tetraethoxysilane): 20 C_2H_5OH:5.4 H_2O:0.004 HCl:0.16 CTAB (cetyltrimethyl ammonium bromide) was dispensed on to a Si(100) substrate. The composition of this sol was known to yield dip-coated films having the 2D hexagonal $p6m$ symmetry. For the slow evaporation technique used in the present measurements, the volume of liquid that was dispensed on the substrate was precisely controlled with a micropipette. Only one drop ($\sim$100 μl) of the initial sol was used so as to wet entirely the surface of the 2 cm^2 silicon wafer. After evaporation, the film was $\sim$100 nm thick. The substrate was placed into the x-ray evaporation cell in which the humidity was controlled by flowing either dry or humid nitrogen. The relative humidity (RH) is defined as the ratio of the partial vapor pressure P of water to the saturation vapor pressure P_0 at that temperature. It was measured with a humidity sensor HC-610 from Ohmic Instruments. Because the typical experiment time was 15 min, it was possible to follow the different phases of the self-assembly process, and to correlate them with RH changes. The measurements were performed on the liquid spectrometer of the X22B beam line at the NSLS (National Synchrotron Light Source, BNL, USA). The sample was kept horizontal during the course of the measurements and the incident beam was deflected by a Ge monochromator so that it impinged at a controlled incident angle on the surface of the liquid film, slightly above the critical external angle of the silicon. The incident wavelength was fixed to 1.576 Å and the scattering was monitored with a MAR USA Inc. charge-coupled device (CCD) 2D detector located 0.735 m away from the sample. The optical interferometry was carried out in reflection under normal incidence with a multiwavelength F30 interferometer from Filmetrics Inc.

The EISA process and the effects of RH cycling are illustrated by the sequence of GISAXS patterns in Fig. 1. The first frame [Fig. 1(a)], acquired in the liquid state, exhibits only a streak at $q_y=0$ which is partially blocked by the beam stop to avoid the intense specular reflection. The surfactant

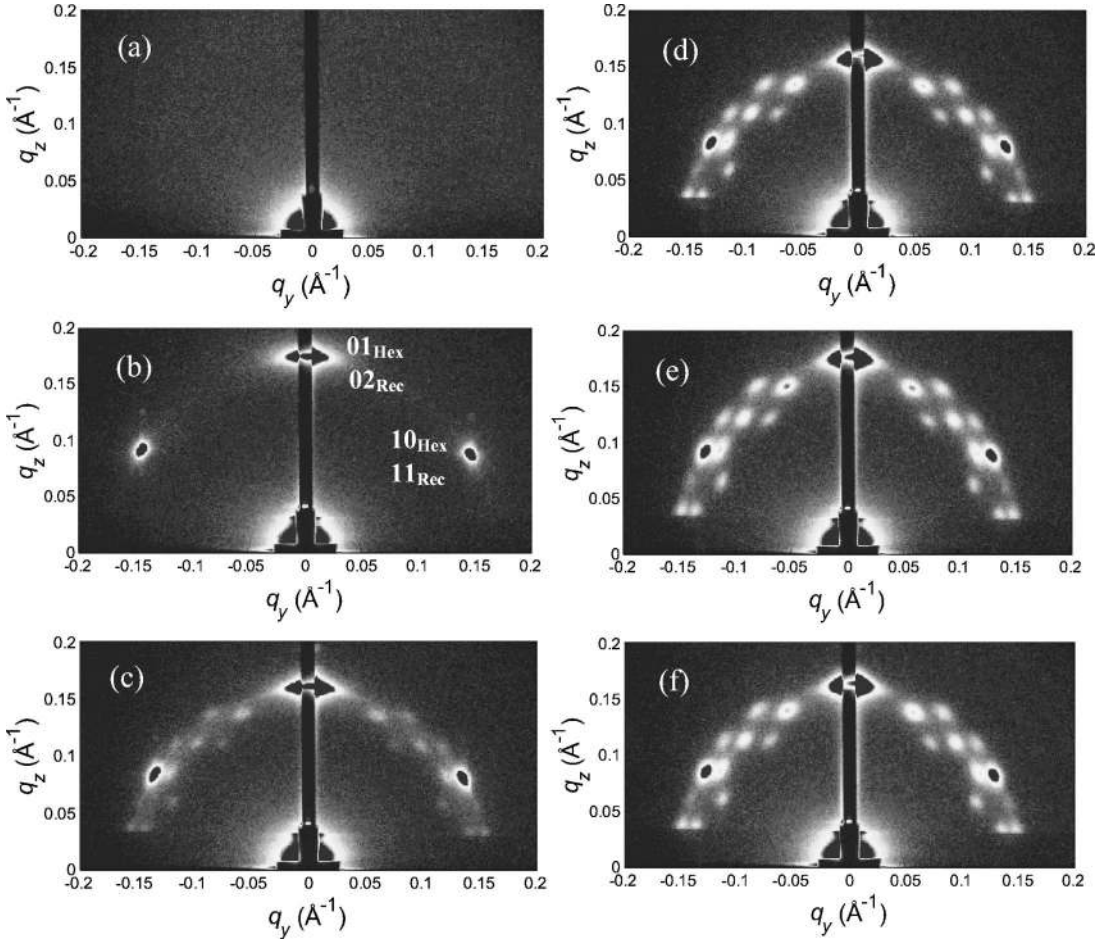

FIG. 1. *In situ* 2D x-ray scattering patterns measured during the chronologic phase transformation of the diluted liquid film to the structured mesophase: (a) liquid phase, (b) 2D hexagonal phase (RH=0.4), (c) 2D hex phase and onset of the cubic phase, (d) 2D hex coexisting with the cubic phase at high humidity (RH=0.8), and (e) distorted 2D hex phase (and the cubic phase) at low humidity (RH =0.3), distorted 2D hex phase (and the cubic phase) at high humidity (RH=0.8). Note, that the 2D detector monitors the reciprocal space along two specific directions that are the q_y direction parallel to the surface of the sample and the q_z direction perpendicular to it (the q_x component is negligible).

molecules are indeed disordered at this high ethanol concentration and the system can be considered as a "diluted liquid phase." The second pattern taken after complete ethanol evaporation shows a 2D hexagonal phase of *p6m* symmetry [Fig. 1(b)]. After about 1 min of evaporation, the 2D hex phase is still fully flexible because the silica network has not yet condensed. At this early stage, the external relative humidity was cycled by flowing alternatively humid or dry nitrogen gas in the cell. Grosso and co-workers define this stage of the process as the MSS (modulable steady state).[9] When the system is still in the MSS, as in Fig. 1(c), we observed that by raising the RH from 40% to 80% the 2D hex phase transforms into the cubic *Pm3n* phase. This transformation is a consequence of the penetration of the water molecules between the charged headgroups of the CTAB molecules. The penetration increases the area occupied by the headgroups and this leads to a decrease in the packing parameter.[14] This change in the packing parameter leads to the transformation of the cylindrical micelles (observed in the 2D hex phase) into spherical ones (in the cubic phase). Further change in the RH mainly affect the lattice parameters as demonstrated by the sequence of GISAXS patterns (Fig. 1). A close look at the position of the Bragg reflection [labeled 01_{Hex} in Fig. 1(b)] shows that at low humidity the reciprocal space is expanded [Figs. 1(b) and 1(e)] while at high humidity it is contracted [Figs. 1(d) and 1(f)]. This effect is directly related to the water intrusion or extrusion upon humidity changes.

In the hexagonal phase, the lattice parameter can be deduced from the location of the $(10)_{Hex}$ or $(01)_{Hex}$ Bragg reflections. The lattice is fairly well described by a unique parameter a_{Hex}=8.29 nm, indicating almost no distortion of the hexagonal network (see Fig. 2). After a period of time, however, the lattice distorts and it is convenient to use a rectangular face-centered unit cell described by two lattice parameters b and c (for details see Refs. 15, 13, and 16). In this two-component rectangular coordinate system $a=b$, the lattice parameter along $\langle 10 \rangle$ is b and along $\langle 01 \rangle$ is c. Further, the $(11)_{rec}$ reflection is equivalent to $(10)_{Hex}$ and the $(02)_{rec}$ reflection is equivalent to $(01)_{Hex}$.

In Fig. 1(c) new peaks emerge which correspond to the cubic phase and this phase coexists with the hexagonal phase. These cubic peaks become more intense in Figs. 1(d)–1(f) but continue to coexist with the hexagonal phase.

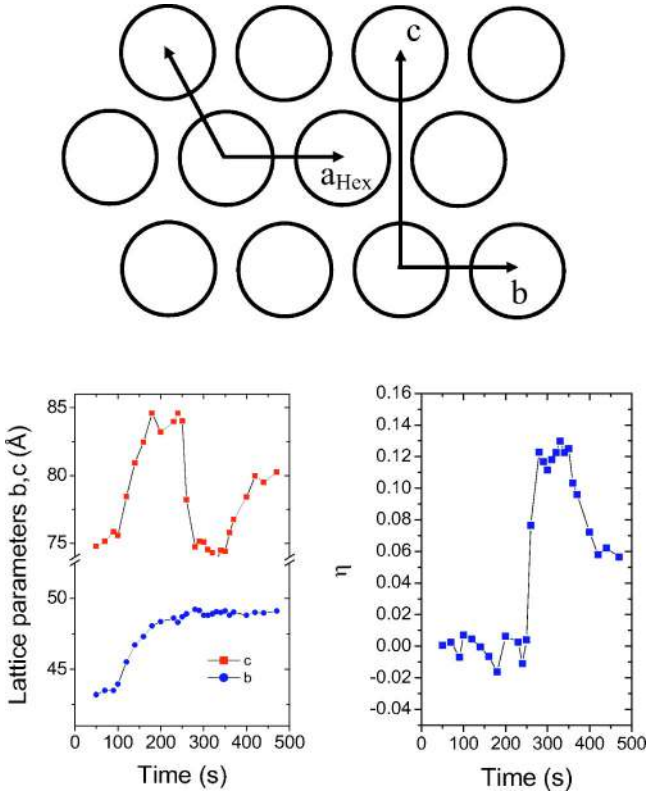

FIG. 2. (Color online) Representation of the 2D hex and rectangular face-centered unit cells (top part). Evolutions of the lattice parameters b and c during humidity cycles (the lattice parameters are derived in the rectangular face-centered unit cell) and of the distortion η as a function of time upon cycling the RH in the cell (bottom part). It is important to note that in reflection geometry, the c lattice parameter can only be evaluated in the framework of the distorted wave Born approximation which takes into account refraction of the beam.

The cubic diffraction pattern consists of three characteristic concentric circles on which the 200, 210, and 211 Bragg reflections are located (for more details about this phase and its indexation see Ref. 13). In Fig. 1(d), the average cubic lattice parameter is $a=b=c=8.96$ nm with the following d spacings $d_{211}=3.68$ nm, $d_{210}=3.99$ nm, and $d_{200}=4.48$ nm. The cubic phase remains stable when the RH is reduced to 30% [see Fig. 1(e)]. By varying the incident angle with respect to the critical angle, thus varying the x-ray penetration depth, we were able to show that the cubic phase was located in the top region of the film, while the bottom region corresponds to the hexagonal phase.

In the following, we describe the changes in the lattice parameters with humidity in the distorted hexagonal phase (see Fig. 2). Although similar effects were also observed in the cubic phase, we have chosen to focus on the distorted-hexagonal phase since it is always present whereas the cubic phase is not. Here we use the rectangular unit cell, introduced above, to describe the distortions since the c/b ratio differs from $\sqrt{3}$, its value for the hexagonal phase. The temporal evolution of the lattice parameters and the distortion from a hexagonal lattice, given by $\eta=(\sqrt{3}-c/b)/\sqrt{3}$, are presented in Fig. 2. In the first period, the RH was maintained at 40% and the hexagonal phase was nearly undistorted. By increasing the humidity, both lattice parameters b and c increase and the distortion remains very weak (up to 250 s in Fig. 2). When the humidity was lowered by introducing dry nitrogen for 250 s $<t<$ 350 s in Fig. 2) the lattice becomes distorted. This is because b was pinned in the direction parallel to the film surface while along the unconstrained z direction the lattice contracts, as shown in Fig. 2 (bottom left panel). We define the pinning effect of the b lattice parameter from the fact that this parameter does not swell or contract during the subsequent RH cycles following the first RH cycle.

The first humidity cycle (up to 250 s in Fig. 2) differs from subsequent cycles. During the first cycle c increased from 7.4 to 8.5 nm whereas b increased from 4.2 to 4.8 nm. Since both lattice constants increased by the same 15% proportion there is no overall change in the shape of the unit cell. Along b, the 0.6 nm increase corresponds directly to the thickness of the water layer surrounding the micelle. Estimating the diameter of water as 0.31 nm from the cube root of the volume of a bulk water molecule, 0.6 nm corresponds to nearly two layers of water, one on each side of the micelle. By considering the 9 nm^2 increase in the area of the unit cell and a 9.6 nm^2 area per water molecule, 94 water molecules of water are needed to hydrate the two micelles per unit length of water. Thus, in the 2D hexagonal plane there are 47 water molecules covering each micelle per unit length of water.

The b lattice parameter versus time, shown in Fig. 2, appears to saturate almost exponentially as if governed by the diffusion-limited process. This curve (not shown) is reasonably well described by an exponential function with a characteristic time constant of 55 s. This time constant corresponds to the time after which the pinning becomes irreversible (in the present experimental condition of RH). After the drying stage we again increased the RH to ~80%. The c lattice parameter was found to rise again from 7.4 to 8.0 nm while at the same time the distortion decreased from 15% to 8%. After the first cycle, the system does not recover its full expansion along the z direction because of the reduced flexibility of the silica network. By cycling over longer periods of time, c increased less and less as the silica network further condensed. During these cycles we also measured the total thickness of the film by optical interferometry at 30% and 80% humidity. The thickness evolved from 980 nm at 80% humidity to 860 nm at 30% humidity. These observations are fully consistent with the corresponding lattice parameter obtained concurrently. This clearly suggests that the entire film swelled and contracted simultaneously. Similar cycling experiments were performed after curing the 2D hexagonal phase for 10 min at RH=40% (not shown). Under these conditions, the 2D hexagonal phase did not transform into a cubic one upon increasing the RH. During the curing process, the c lattice parameter remained almost constant at 7.4 nm whereas the b lattice parameter increased slightly from 4.6 to 4.75 nm. Compared to the same experiment made at higher RH, one can clearly observe that the b lattice parameter was pinned to a much lower value. This demonstrated that the in-plane lattice parameter can be tuned to a given value by adjusting the RH in the very early modulated stages of organization. After more than 10 min of

curing, lowering the RH caused the *c* lattice parameter to decrease from 7.4 to 6.6 nm with no concomitant change of the *b* lattice parameter. Increasing the RH recovered the initial value of the *c* parameter.

Our observations clearly demonstrate that the directions parallel and perpendicular to the surface are not equivalent with respect to water intrusion and extrusion, especially after the first initial flexible regime. The modulable steady state (MSS) can therefore be decomposed into a fully flexible state (FFS) followed by an in-plane frozen state (IPFS). In the IPFS, only the *c* lattice parameter varies with RH. This change steadily diminishes as a function of time indicating the evolution of the degree of condensation of the silica network. This naturally raises the issue of why the network remains flexible along the surface-normal direction while frozen in-plane. Our lattice constant results shows that water enters the film at the air-film interface and quickly diffuses through the film from this interface. In part this is supported by the coexistence of the cubic and 2D hexagonal phases which coexist epitaxially above each other and the interferometric measurements. The diffusion of water is likely made through porous channels that are either located in the silica matrix (micropores) or more likely at the grain boundary between the large numbers of microdomains covering the surface. During water intrusion, the increase of *c* is only possible if the silica network is flexible. This flexibility should also permit in-plane changes of *b*. Therefore the anisotropic pinning effect is probably not related to the condensation of the silica network only. Indeed there is no reason why the silica network should be more condensed in-plane than perpendicular to the surface. Therefore we believe that the anisotropic behavior of the lattice parameter is more related to the coexistence of a patchwork of domains designed during the formation of the surfactant cylindrical rods. For simplicity let us consider a set of orthogonal domains as shown in Fig. 3. Arrows indicate the directions in which silica can expand or contract during RH cycling (these directions are the perpendicular directions to the cylinder axis). As the middle domain is trapped between two adjacent domains in which the silica matrix cannot expand along the same in-plane direction, the middle domain will be pinned in-plane. It appears from our explanation that the pinning effect is mostly related to the different orientations taken by the cylinders during their formation and to the subsequent formation of domains at the surface. It is important to note that this effect is not related to existence of the cubic phase. Indeed complementary experiments have shown that a similar effect can be observed in a film having the 2D hex symmetry only.[17]

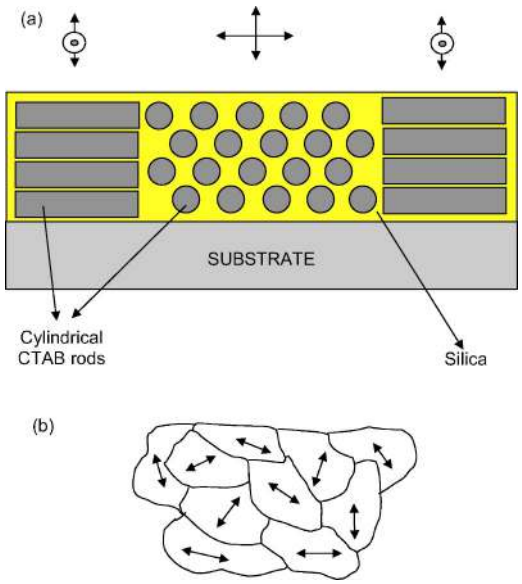

FIG. 3. (a) Schematic representation of a set of three hexagonal domains with their cylindrical axis perpendicular to each other. The arrows indicate the direction of expansion or contraction of the silica network. The middle domain is imprisoned between two adjacent domains. (b) Top view of the domains patchwork with an arrow indicating the direction of deformation of the silca network.

In summary, for the CTAB-silica films investigated during RH cycling in the present study there is quantitative agreement between the atomic-scale lattice constant and the total film thickness. The former is obtained from GISAXS and the latter with interferometry measurements. We found that water uptake during FFS corresponds to one water molecule layer for each micelle. In the following IPFS, this behavior is impeded by both the progressive condensation of the silica network and by the pinning effect. The lattice distortion upon water intercalation is due to the anisotropic extension in lateral and normal direction, which is consistent with the pinning effect explanation. The latter one is, presumably, due to the existence of domains of different orientations at the surface of the film.

This work was supported by the French ACI "Nanostructure" under project No. 03-01 and the French ACI "Nanoporomat." Work at Brookhaven National Laboratory is supported by U.S. DOE Contract No. DE-AC02-98CH10886.

[1] J. S. Beck *et al.*, J. Am. Chem. Soc. **114**, 10834 (1992).
[2] C. T. Kresge *et al.*, Nature (London) **359**, 710 (1992).
[3] C. J. Brinker *et al.*, Adv. Mater. (Weinheim, Ger.) **11**, 579 (1999).
[4] Y. Lu *et al.*, Nature (London) **398**, 223 (1999).
[5] Y. Lu *et al.*, Nature (London) **389**, 364 (1997).
[6] S. A. Bagshaw, E. Prouzet, and T. J. Pinnavaia, Science **269**, 1242 (1995).
[7] D. P. Zhao *et al.*, Chem. Commun. (Cambridge) **7**, 2499 (1998).
[8] D. Zhao *et al.*, Adv. Mater. (Weinheim, Ger.) **16**, 1380 (1998).
[9] D. Grosso *et al.*, Chem. Mater. **13**, 1848 (2001); **14**, 931 (2002).
[10] F. Cagnol *et al.*, J. Mater. Chem. **13**, 61 (2003).
[11] E. Crepaldi *et al.*, J. Am. Chem. Soc. **125**, 9770 (2003).
[12] A. Gibaud *et al.*, in *Studies in Surface Science and Catalysis*, edited by S. E. Park *et al.* (Elsevier, New York, 2003), Vol. 146, pp. 351–354.
[13] A. Gibaud *et al.*, J. Phys. Chem. B **107**, 6114 (2003).
[14] J. Israelachvili, in *Intermolecular and Surface Forces*, 2nd ed. (Academic Press, London, 1992).
[15] D. A. Doshi *et al.*, J. Am. Chem. Soc. **125**, 11646 (2003).
[16] D. A. Doshi *et al.*, J. Phys. Chem. B **107**, 7683 (2003).
[17] S. Dourdain *et al.*, Physica B (to be published).